



Published in final edited form as:

Mater Sci Eng C Mater Biol Appl. 2018 April 01; 85: 79–87. doi:10.1016/j.msec.2017.12.008.

Biomimetic Polyurethane/TiO₂ Nanocomposite Scaffolds Capable of Promoting Biomineralization and Mesenchymal Stem Cell Proliferation

Qingxia Zhu^{1,2}, Xiaofei Li¹, Zhaobo Fan¹, Yanyi Xu¹, Hong Niu¹, Chao Li¹, Yu Dang¹, Zheng Huang¹, Yun Wang³, and Jianjun Guan¹

¹Department of Materials Science and Engineering, The Ohio State University, 2041 College Road, Columbus, OH 43210, USA

²Department of Materials Science and Engineering, Jingdezhen ceramic institute, Jiangxi 333001, China

³Division of Periodontology, The Ohio State University, 305 W. 12th Avenue, Columbus, OH 43210, USA

Abstract

Scaffolds with extracellular matrix-like fibrous morphology, suitable mechanical properties, biomineralization capability, and excellent cytocompatibility are desired for bone regeneration. In this work, fibrous and degradable poly(ester urethane)urea (PEUU) scaffolds reinforced with titanium dioxide nanoparticles (nTiO₂) were fabricated to possess these properties. To increase the interfacial interaction between PEUU and nTiO₂, poly(ester urethane) (PEU) was grafted onto the nTiO₂. The scaffolds were fabricated by electrospinning and exhibited fiber diameter of <1 μm. SEM and EDX mapping results demonstrated that the PEU modified nTiO₂ was homogeneously distributed in the fibers. In contrast, severe agglomeration was found in the scaffolds with unmodified nTiO₂. PEU modified nTiO₂ significantly increased Young's modulus and tensile stress of the PEUU scaffolds while unmodified nTiO₂ significantly decreased Young's modulus and tensile stress. The greatest reinforcement effect was observed for the scaffold with 1:1 ratio of PEUU and PEU modified nTiO₂. When incubating in the simulated body fluid over an 8-week period, biomineralization was occurred on the fibers. The scaffolds with PEU modified nTiO₂ showed the highest Ca and P deposition than pure PEUU scaffold and PEUU scaffold with unmodified nTiO₂. To examine scaffold cytocompatibility, bone marrow-derived mesenchymal stem cells were cultured on the scaffold. The PEUU scaffold with PEU modified nTiO₂ demonstrated significantly higher cell proliferation compared to pure PEUU scaffold and PEUU scaffold with unmodified nTiO₂. The above results demonstrates that the developed fibrous nanocomposite scaffolds have potential for bone tissue regeneration.

Corresponding Author: Jianjun Guan, Ph.D. Associate Professor, Department of Materials Science and Engineering, The Ohio State University, 2041 College Road, Columbus, OH 43210, Phone: 614-292-9743, guan.21@osu.edu.

Publisher's Disclaimer: This is a PDF file of an unedited manuscript that has been accepted for publication. As a service to our customers we are providing this early version of the manuscript. The manuscript will undergo copyediting, typesetting, and review of the resulting proof before it is published in its final citable form. Please note that during the production process errors may be discovered which could affect the content, and all legal disclaimers that apply to the journal pertain.

Keywords

nanocomposite; polyurethane; TiO₂ nanoparticle; mesenchymal stem cells; biocompatibility

1. Introduction

Self-regeneration of critical size bone defects caused by trauma, tumor removal, and infection remains challenging in clinical settings. [1–3] Scaffolds have been widely used to aid the regeneration. A typical scaffold should have appropriate porosity to allow cell ingrowth, be osteoconductive, and possess suitable mechanical properties. [1–3] Among different types of scaffolds, those mimicking the properties of bone tissue extracellular matrix (ECM) have been considered as promising candidates.[4–7] These scaffolds can accelerate the regeneration by preventing fibrous encapsulation, promoting osseointegration, and stimulating cell infiltration, proliferation and osteogenic differentiation. [4–8]

Bone is a hard tissue that also has high toughness and tensile strength. To fabricate scaffolds with suitable toughness, flexible polymers such as polyurethane and polycaprolactone can be used. [9–44] The resulting scaffolds generally have higher toughness than those based on stiffer polymers such as polylactide and polyglycolide. Biodegradable polyurethane is a class of polymer that has attracted great attention in the biomaterials community due to its excellent biocompatibility and robust mechanical properties. Porous thermoplastic and thermoset polyurethane scaffolds have been utilized for bone regeneration in animal and preclinical studies. [9–29] The scaffolds with tailored chemical and mechanical properties can promote osteogenic cells to populate and differentiate within the scaffolds, thus stimulating bone regeneration.[25–29] To further augment the regeneration, growth factors such as BMP-2 and PDGF have been loaded into polyurethane scaffolds.[28, 45–47] One of the limitations for biodegradable polyurethane scaffolds is that their modulus and tensile strength are much lower than those of the bone tissue. Increasing these properties is expected to make polyurethane scaffolds more suitable for bone regeneration. An effective approach is to use stiffer soft segment during the synthesis. For example, replacing polycaprolactone with polyhydroxybutyrate can largely increase polyurethane Young's modulus and tensile strength.[48–52] However, this approach may simultaneously compromise toughness of the polymers.

Polyurethane composite scaffolds may retain toughness of the polyurethane while increasing modulus and tensile strength. Microspheres and nanoparticles can be incorporated into polyurethane scaffolds during the fabrication, such as hydroxyapatite,[14, 53, 54] carbon nanotubes,[55–57] and titanium dioxide (TiO₂). [58, 59] These inorganic materials are much stronger and stiffer than polymers. Compared to microspheres, nanoparticles may better reinforce polyurethanes because of their higher surface area-to-volume ratio.[60] TiO₂ nanoparticles are attractive for polymer reinforcement especially in dental applications.[61–63] These nanoparticles have good biocompatibility and antibacterial property.[61–63] In addition, they can suppress immune response which commonly occurs after scaffold implantation.[64] In this work, we took advantage of these properties to fabricate TiO₂ nanoparticles-reinforced polyurethane scaffolds. A major limitation of using unmodified

TiO₂ nanoparticles to reinforce polymers is the uneven distribution, which compromises the reinforcement effect.[65] In addition, the nanoparticles may readily leach out from the scaffolds when their interactions with polymers are weak. [65] The released nanoparticles may be intaken by cells causing potential damage.[66] To address these limitations, approaches such as surface modification of TiO₂ nanoparticles, [65] and increase of polymer polarity [67] have been developed to augment the physical interactions of the nanoparticles and polymers. In this work, we hypothesized that chemical conjugation of polymers to the TiO₂ nanoparticles can better increase the interactions than simply modifying either the nanoparticles or polymers, thus efficiently increasing scaffold modulus and tensile strength, and decreasing nanoparticle release.

Bone tissue ECM is a nanocomposite consisting of collagen fibers and hydroxyapatite nanoparticles. Thus, scaffolds with fibrous morphology and biomineralization capability are desired for bone regeneration. To fabricate scaffolds with fibrous morphology, commonly used techniques include thermally induced phase separation,[68–71] and electrospinning. [72–75] Thermally induced phase separation technique generates fibers with diameter ranging from few to 100 nm depending on the phase separation temperature and solution concentration. [68–71] Electrospinning of polymer solution is a more convenient approach to fabricate fibrous scaffolds. The resulting scaffolds typically have fiber diameters in the range of 10–1000 nm, within the range of fibrous ECM. [72–75] A major advantage of electrospinning is that reinforcement nanoparticles can be readily incorporated into the fibers during fabrication by mixing with polymer solutions.[76] In this work, we electrospun polyurethane scaffolds with TiO₂ nanoparticles in the fibers. Previous study demonstrated that TiO₂ surface with nanostructure has the ability to promote apatite formation.[8] It is hypothesized that the TiO₂ nanoparticles impart the scaffolds with biomineralization capability. We investigated the capability of TiO₂ nanoparticles in improving scaffold mechanical properties, promoting biomineralization, and supporting osteogenic cell proliferation.

2. Materials and methods

2.1. Materials

All chemicals were purchased from Sigma-Aldrich unless otherwise stated. Hexamethylene diisocyanate (HMDI) was purified by vacuum distillation. Polycaprolactone (PCL) diol with an average molecular weight of 2000 g/mol, and dimethylolpropionic acid (DMPA) were vacuum dried overnight at 60°C before use. TiO₂ nanoparticles comprised of 50% anatase and 50% rutile crystal forms. The average particle size and purity were 21 nm and 99.9%, respectively. Anhydrous toluene, dimethylformamide (DMF), and isopropanol were used as received.

2.2. Functionalization of TiO₂ nanoparticles with reactive hydroxyl groups

TiO₂ nanoparticles were reacted with DMPA to introduce hydroxyl groups (Scheme 1) following a previous report.[65] DMPA was dissolved in 2-propanol. The nanoparticles were then dispersed in the DMPA solution. After ultrasonic agitation for 5 min, the mixture was reacted at 80°C for 12 h under constant stirring with the protection of nitrogen gas. The

molar ratio of DMPA to nTiO₂ was controlled at 2.4. After reaction, the nanoparticles were collected by centrifugation at 10000 rpm, and then washed with methanol for 3 times to remove the unreacted DMPA.

2.3 Synthesis of poly(ester urethane) (PEU) grafted TiO₂, and poly(ester urethane)urea (PEUU)

The PEU grafted TiO₂ nanoparticles (PEU-g-nTiO₂) were synthesized by a two-step approach (Scheme 2). In the first step, HMDI and PCL diol were dissolved in a mixture of DMF/toluene at 1:1 volume ratio. The molar ratio of HMDI and PCL diol was 2:1. Stannous octoate was then added. The reaction was conducted at 85°C for 2 h with the protection of nitrogen gas. In the second step, the DMPA functionalized nTiO₂ was added to the above solution. The molar ratio of HMDI and the functionalized nTiO₂ was 1:1. The reaction was conducted at 80°C for 4 h. The mixture was then centrifuged followed by washing with DMF/toluene for 3 times. The PEU-g-nTiO₂ was finally vacuum dried at 40°C. To confirm the conjugation of PEU, the material was characterized by FT-IR.

PEUU was synthesized using PCL as soft segment, and HMDI and putrescine as hard segment following our established protocols.[75, 77] The molar ratio of PCL diol, HMDI and putrescine was controlled at 1/2/1. In brief, PCL diol was dissolved in DMSO to form a solution. HMDI was then added under the protection of nitrogen gas. After addition of stannous octoate, the reaction was conducted at 80°C in an oil bath for 3 h to form prepolymer. The solution was cooled down to room temperature. Putrescine solution in DMSO was then added dropwise to the prepolymer solution for chain extension. The mixture was stirred at room temperature overnight. The polymer solution was precipitated in cold NaCl solution. After immersing in the DI water for 24 h, the polymer was vacuum dried at 60°C.

2.4. Fabrication of fibrous PEUU scaffolds reinforced with PEU-g-nTiO₂

The fibrous scaffolds were fabricated by electrospinning. PEUU was dissolved in 1,1,1,3,3,3-hexafluoro-2-propanol (HFIP) to form a 6% solution. PEU-g-TiO₂ was then added to the solution. The mixture was sonicated to allow particles to uniformly distribute in the solution. The ratio of PEUU and PEU-g-TiO₂ was controlled at 1/1, 1/2, and 2/1 wt%, respectively. The mixture was charged at +15 kv. The flow rate was 1 ml/h. The fibers were collected on a rotating mandrel with rotation speed of 1000 rpm, and charged at -10 kv. The resulting scaffolds (abbreviated as PEU-g-TiO₂/PEUU) had a thickness of ~100 μm. Pure PEUU scaffold, and PEUU scaffold with unmodified TiO₂ nanoparticles (ratio of 1:1, abbreviated as nTiO₂/PEUU) were also fabricated to serve as controls.

2.5 Characterization of PEUU scaffolds reinforced with PEU-g-nTiO₂

Morphology of the scaffolds was characterized by a LEO 1530 scanning electron microscopy (SEM). The bulk composition was analyzed using energy-dispersive x-ray spectroscopy (EDX) attached to the SEM. FT-IR spectra were recorded on a Nicolet Magna-IR 750 spectrometer. To measure mechanical properties, dog bone-shaped die with ~20 mm gauge length and ~2 mm gauge width were used to cut 4–5 specimens from each scaffold. The specimens were immersed in 37°C water for 24 h before test. The tensile testing was

performed on a TestResources 1000R load frame (model 1322) equipped with a 222.4 N load cell and a 37°C water bath. [75, 77] A cross-head speed of 10 mm/min was used.

2.6 Biomineralization of PEUU scaffolds reinforced with PEU-g-nTiO₂

PEUU, nTiO₂/PEUU, and PEU-g-nTiO₂/PEUU scaffolds were used for the assessment of biomineralization property. The samples were weighted and then immersed in a simulated body fluid (SBF) at 37°C. SBF was prepared by dissolving 10.806 g NaCl, 0.852 g Na₂CO₃, 1.008 g NaHCO₃, 0.144 g Na₂SO₄, 0.450 g KCl, 0.351 g K₂HPO₄, 0.622 g MgCl₂·6H₂O, 200 ml of 0.2 M NaOH solution, and 0.586 g CaCl₂ and 34.784 g HEPES in 1 L of DI water. [78] The inorganic ion concentrations in SBF were equal to those of human blood plasma. [78] After 1, 2, 4, and 8 weeks of incubation, samples (n=5 for each scaffold type at each time point) were collected, freeze dried, and weighted. Weight change was then quantified. To confirm the biomineralization, EDX was used to characterize the scaffolds.

2.7. Mesenchymal stem cell growth on PEUU scaffolds reinforced with PEU-g-nTiO₂

To evaluate the ability of PEUU scaffolds reinforced with PEU-g-nTiO₂ to support cell growth, rat bone marrow-derived mesenchymal stem cells (MSCs) were seeded on the scaffolds. PEUU and nTiO₂/PEUU scaffolds were used as controls. MSCs were cultured in a T-175 flask using Dulbecco's Modified Eagle Medium (DMEM) supplemented with 20% FBS, 2% l-glutamine and 1% penicillin/streptomycin as culture medium.[79, 80] The scaffolds were punched into 6 mm diameter disks. After sterilizing under UV irradiation for 1 h in a laminar flow hood, the disks were placed in a 96-well tissue culture plate. MSCs were seeded onto each disk at a density of 2×10^5 cells/ml. After 1, 3, and 7 days of culture under normal conditions (21% O₂, 5% CO₂), double-stranded DNA (dsDNA) content of the live cells in each sample was measured using PicoGreen assay (Invitrogen).[79, 80]

2.8. Statistical analysis

One way ANOVA test was utilized for data analysis. Data were presented as mean \pm standard deviation. Statistical significance was defined as $p < 0.05$.

3. Results and discussion

3.1. Synthesis of PEU-g-nTiO₂

TiO₂ nanoparticle was first functionalized with DMPA to introduce hydroxyl groups onto the surface before grafting PEU. These hydroxyl groups can readily react with isocyanate groups. The reaction of DMPA and nTiO₂ is occurred between carboxyl groups of DMPA and Ti of nTiO₂ by forming bidentate chelating type coordination bonding. [81] To graft PEU onto the functionalized TiO₂ nanoparticles, PEU prepolymer with isocyanate groups was first prepared by reacting PCL diol with HMDI at a molar ratio of 1:2. The use of PCL allows the PEU to be degradable. Successful synthesis of PEU-g-nTiO₂ was confirmed by FTIR spectrum that exhibited characteristic peaks of PEU and TiO₂ (Figure 3). The absorption at 643 cm⁻¹ is from nTiO₂. The carbonyl peak at 1725 cm⁻¹ is from urethane group. All of the isocyanate groups in the prepolymer were reacted with hydroxyl groups introduced onto the nTiO₂ surface since there is no isocyanate peak at 2265cm⁻¹. Consistent with previous report, [65] the coordination bonding between DMPA and nTiO₂ is not

obvious in the spectrum, possibly because the absorption level of Ti–O–C coordination is significantly small compared to that of the bonds in PEU.

3.2. Fibrous nanocomposite scaffold fabrication

Fibrous scaffolds based on PEUU and PEU-g-nTiO₂ were fabricated by electrospinning. The PEUU was synthesized using the same soft segment and diisocyanate as PEU. Our previous study demonstrated that this polymer supported the growth of cardiosphere-derived cells. [75] HFIP was used as a solvent for PEUU. The benefit of using this high polarity solvent is that it allowed PEU-g-nTiO₂ to evenly and stably suspend in the PEUU solution, thus facilitating the fabrication of fibers with uniform distribution of nTiO₂.

The fabricated PEUU scaffold without nTiO₂ or PEU-g-nTiO₂ assumed smooth fibers with a diameter less than 1 μm (Figure 4a). The scaffolds based on unmodified nTiO₂ and PEUU (nTiO₂/PEUU) exhibited both fibers and beads (Figure 4b). EDX analysis was performed to determine the distribution of nTiO₂. Figure 5 demonstrated that nanoparticles were not uniformly distributed in the scaffolds, and beads were nanoparticle aggregation. It is likely that unmodified nTiO₂ aggregated during the fabrication due to poor interactions between nTiO₂ and PEUU. The modification of nTiO₂ with PEU (PEU-g-nTiO₂) increased the interfacial interaction of the nanoparticles and PEUU. This allowed nanoparticles to stably suspend in the solution during scaffold fabrication. As a result, the scaffolds contained only fibers without beads (Figure 4d–e). EDX analysis confirmed that nanoparticles were evenly distributed in the scaffolds (Figure 5). Scaffold fiber morphology was dependent on the ratio of PEU-g-nTiO₂ to PEUU. When the ratio was 1:2, the fibers were smooth. The increase of the ratio to 1:1 and 2:1 led to forming more rough fibers (Figure 4e).

3.3 Scaffold mechanical properties

One of the purposes in using nTiO₂ is to reinforce the PEUU scaffolds thus increasing both Young's modulus and tensile strength for improved performance during bone regeneration. The pure PEUU scaffold had Young's modulus and tensile strength of 31.8±2.3 and 34.3±0.9, respectively. Simply mixing unmodified nTiO₂ and PEUU (nTiO₂/PEUU scaffold) did not show reinforcement effect. Instead, both Young's modulus and tensile strength were significantly decreased compared with PEUU scaffold ($p < 0.001$). This is likely due to the low interfacial interaction between nTiO₂ and PEUU. It led to the aggregation of nTiO₂ in the solution during the scaffold fabrication process. The scaffolds therefore had nTiO₂ aggregates attached to the fibers (Figure 4b and Figure 5a), which cannot efficiently dissipate external force. For those nanoparticles that are in the fibers, even they can disperse uniformly, the weak interfacial interaction between PEUU cannot effectively reinforce the scaffold.

Modification of nTiO₂ with PEU (PEU-g-nTiO₂) can increase its interfacial interaction with PEUU because of the strong hydrogen bonding between urethane groups and urethane-urea groups in both polymers. This resulted in the reinforcement effect. Figure 6 demonstrated that adding PEU-g-nTiO₂ into the PEUU scaffolds significantly increased Young's modulus compared to the pure PEUU scaffold when the ratio of PEU-g-nTiO₂ and PEUU was ranged from 1:2 to 2:1 ($p < 0.01$). The highest Young's modulus was for the scaffold with the ratio of

1:1 where it was 48.8 ± 3.2 MPa, a 53.5% of increase over pure PEUU scaffold. For the tensile strength, the scaffolds with PEU-g-nTiO₂/PEUU ratios of 1:2 and 1:1 were significantly higher than pure PEUU scaffold ($p < 0.05$) while the scaffold with the ratio of 2:1 showed similar value. The decrease of Young's modulus and tensile strength when the PEU-g-nTiO₂/PEUU ratio was increased from 1:1 to 2:1 is probably attributed to the decrease of interfacial interaction between PEUU and PEU when the content of PEU-g-nTiO₂ is higher than PEUU. It is also possible that PEU-g-nTiO₂ cannot efficiently distribute in the PEUU fibers when its content is high. Similar trend was found for collagen scaffolds reinforced with carbon nanotubes.[82]

3.4 Scaffold biomineralization

Biomineralization is critical during bone regeneration. Scaffolds capable of stimulating biomineralization may be able to promote the regeneration. [8] The developed fibrous scaffolds have high surface-area-to-volume ratio, thus may facilitate the biomineralization. To investigate the biomineralization capability of TiO₂ nanoparticles reinforced PEUU scaffold, PEU-g-nTiO₂/PEUU=1:1 was used since it had the highest Young's modulus. The scaffold was incubated in SBF for 8 weeks. Controls were PEUU and nTiO₂/PEUU scaffolds. All scaffolds showed slight weight loss after 1 week of incubation ($p > 0.05$ for each scaffold). It is possible that PEUU degradation-induced weight loss is greater than biomineralization-induced weight gaining during this period. The PEUU scaffold exhibited continuous weight loss for 4 weeks. Significant net weight gaining was observed only after 8 weeks ($p < 0.05$, week 4 vs. week 8), indicating that biomineralization was dominated for PEUU after 4 weeks. The nTiO₂/PEUU scaffold demonstrated net weight gaining after 4 weeks, earlier than PEUU scaffold. After 8 weeks of incubation, the scaffold gained ~13% of weight, significantly greater than the original weight ($p < 0.05$, week 0 vs. week 8). These results suggest that TiO₂ nanoparticles in the scaffold accelerated the biomineralization. This is consistent with previous studies where TiO₂ containing materials promoted the absorption of Ca²⁺ and PO₄³⁻. [83]

The PEU-g-nTiO₂/PEUU scaffold showed net weight gaining only after 2 weeks of incubation, sooner than nTiO₂/PEUU scaffold. After 8 weeks, the net weight gaining was 10% ($p < 0.05$ for weight of week 0 vs. weight of week 8). The Ca and P containing ions were deposited uniformly in the PEU-g-nTiO₂/PEUU scaffold (Figure 8), attributing to the even distribution of TiO₂ nanoparticles (Figure 5). Elemental content of Ca and P analyzed from EDX mapping is listed in Table 1. Consistent with weight change results in Figure 7, the PEU-g-nTiO₂/PEUU scaffold had the highest Ca and P deposition. In addition, the nTiO₂/PEUU scaffold demonstrated greater Ca and P deposition than PEUU scaffold. The above results suggest that PEU modification stimulated nTiO₂ biomineralization. The PEU grafted onto the nanoparticles is based on polycaprolactone and HMDI. The chain length of PEU should be shorter than that of PEUU as no chain extension reaction was performed for it. Therefore, PEU possibly degraded faster than PEUU. The hydrolysis of PCL chain may leave -COOH groups on the nTiO₂ surface, which then attract cationic species like Ca²⁺ to deposit.

3.5 Mesenchymal stem cell growth on scaffolds

Scaffolds for bone regeneration can be implanted alone to allow endogenous cells including osteoblasts and stem cells to induce regeneration. They can also be transplanted together with osteogenic cells to direct the regeneration. In both approaches, it is necessary for the scaffolds to support cell proliferation. To investigate the capability of PEU-g-nTiO₂/PEUU scaffold to supporting cell growth, bone marrow-derived MSCs were seeded on the scaffold of PEU-g-nTiO₂/PEUU=1:1 since it had the highest Young's modulus. PEUU and nTiO₂/PEUU scaffolds were used as controls. Bone marrow-derived MSCs are known for their ability to promote bone regeneration. Cell dsDNA (for live cells) content was monitored during the culture. Figure 9 demonstrated that MSC dsDNA content was increased on all 3 scaffolds during the 7-day culture period. The highest increase was found for PEU-g-nTiO₂/PEUU scaffold where dsDNA content was 2.5 and 9.9 folds of day 1 at days 3 and 7, respectively ($p < 0.01$ for day 3 vs. day 1, and day 7 vs. day 3). The nTiO₂/PEUU scaffold and PEUU scaffold exhibited similar levels of dsDNA increase at day 7 ($p < 0.05$ for day 7 vs. day 1 for both scaffolds). The above results demonstrate that incorporation of PEU modified TiO₂ nanoparticles into PEUU scaffold improved MSC proliferation while incorporation of unmodified TiO₂ nanoparticles did not. It is possible that PEU on the nanoparticle surface augmented its hydrophilicity, thus increasing its interaction with cells. Our future work will explore how scaffold properties such as TiO₂ content, fiber diameter, and single fiber modulus can be tuned to induce the differentiation of MSCs into osteogenic phenotype.

One of the concerns for using TiO₂ nanoparticles is that the released nanoparticles may be toxic to bone cells. [66] For example, TiO₂ nanoparticles with size of 15 nm have been shown to impair SOD1 and SOD2 secretion and promote ROS generation after intaking by osteoblasts. [84] TiO₂ nanoparticles can also change the ultrastructure of cells. [84] In this work, the PEU modified TiO₂ nanoparticles may not be readily released from the PEUU fibers due to increased interaction between the nanoparticles and PEUU. In addition, the PEU modified TiO₂ nanoparticles may not be easily intaken by the cells even after PEU and PEUU are degraded. Biomineralization study demonstrated that the modified nanoparticles promoted mineral deposition, which can increase the size of the nanoparticles to an extent that cells cannot readily intake.

4. Conclusion

Fibrous PEUU scaffolds reinforced with TiO₂ nanoparticles were fabricated for bone regeneration. Unmodified TiO₂ nanoparticles cannot uniformly distribute in the fibers, and did not show reinforcement effect. The PEU modified nanoparticles can evenly distribute in the fibers, and significantly increased scaffold Young's modulus and tensile strength. The scaffolds based on modified TiO₂ nanoparticles and PEUU exhibited greater biomineralization capability than PEUU scaffold. In addition, these scaffolds better promoted MSC growth than pure PEUU scaffold and PEUU scaffold with unmodified TiO₂ nanoparticles. These scaffolds alone or combined with osteogenic cells have the potential for bone regeneration.

Acknowledgments

This work was supported by US National Institutes of Health (R01HL138353, R01EB022018, R01AG056919, and R21EB021896), US National Science Foundation (1708956), National Science Foundation of China (81471788 and 51462014), Young Scientists of Jiangxi Province (20122BCB23019), “2014 Oceangoing Voyage” from Jiangxi Science and Technology Association, and China Scholarship Council (P-1-00577).

References

1. Mardas N, Dereka X, Donos N, Dard M. Experimental model for bone regeneration in oral and cranio-maxillo-facial surgery. *Journal of investigative surgery : the official journal of the Academy of Surgical Research*. 2014; 27:32–49. [PubMed: 23957784]
2. Short AR, Koralla D, Deshmukh A, Wissel B, Stocker B, Calhoun M, Dean D, Winter JO. Hydrogels That Allow and Facilitate Bone Repair, Remodeling, and Regeneration. *Journal of materials chemistry B, Materials for biology and medicine*. 2015; 3:7818–7830. [PubMed: 26693013]
3. van Griensven M. Preclinical testing of drug delivery systems to bone. *Advanced drug delivery reviews*. 2015; 94:151–164. [PubMed: 26212157]
4. Neel, EA Abou, Bozec, L., Knowles, JC., Syed, O., Mudera, V., Day, R., Hyun, JK. Collagen-emerging collagen based therapies hit the patient. *Advanced drug delivery reviews*. 2013; 65:429–456. [PubMed: 22960357]
5. Ferreira AM, Gentile P, Chiono V, Ciardelli G. Collagen for bone tissue regeneration. *Acta biomaterialia*. 2012; 8:3191–3200. [PubMed: 22705634]
6. Li N, Song J, Zhu G, Li X, Liu L, Shi X, Wang Y. Periosteum tissue engineering-a review. *Biomaterials science*. 2016; 4:1554–1561. [PubMed: 27722242]
7. Raucci MG, Guarino V, Ambrosio L. Biomimetic strategies for bone repair and regeneration. *Journal of functional biomaterials*. 2012; 3:688–705. [PubMed: 24955638]
8. Gerhardt LC, Jell GM, Boccaccini AR. Titanium dioxide (TiO₂) nanoparticles filled poly(D,L lactid acid) (PDLA) matrix composites for bone tissue engineering. *Journal of materials science. Materials in medicine*. 2007; 18:1287–1298. [PubMed: 17211724]
9. Giannitelli SM, Basoli F, Mozetic P, Piva P, Bartuli FN, Luciani F, Arcuri C, Trombetta M, Rainer A, Licoccia S. Graded porous polyurethane foam: a potential scaffold for oro-maxillary bone regeneration. *Materials science & engineering. C. Materials for biological applications*. 2015; 51:329–335. [PubMed: 25842142]
10. Gogoi S, Maji S, Mishra D, Devi KS, Maiti TK, Karak N. Nano-Bio Engineered Carbon Dot-Peptide Functionalized Water Dispersible Hyperbranched Polyurethane for Bone Tissue Regeneration. *Macromolecular bioscience*. 2017; 17
11. Kai D, Prabhakaran MP, Chan BQ, Liow SS, Ramakrishna S, Xu F, Loh XJ. Elastic poly(epsilon-caprolactone)-polydimethylsiloxane copolymer fibers with shape memory effect for bone tissue engineering. *Biomedical materials (Bristol, England)*. 2016; 11:015007.
12. Mi HY, Palumbo S, Jing X, Turng LS, Li WJ, Peng XF. Thermoplastic polyurethane/hydroxyapatite electrospun scaffolds for bone tissue engineering: effects of polymer properties and particle size. *Journal of biomedical materials research Part B, Applied biomaterials*. 2014; 102:1434–1444.
13. Pirvu T, Blanquer SB, Benneker LM, Grijpma DW, Richards RG, Alini M, Eglin D, Grad S, Li Z. A combined biomaterial and cellular approach for annulus fibrosus rupture repair. *Biomaterials*. 2015; 42:11–19. [PubMed: 25542789]
14. Selvakumar M, Pawar HS, Francis NK, Das B, Dhara S, Chattopadhyay S. Excavating the Role of Aloe Vera Wrapped Mesoporous Hydroxyapatite Frame Ornamentation in Newly Architected Polyurethane Scaffolds for Osteogenesis and Guided Bone Regeneration with Microbial Protection. *ACS applied materials & interfaces*. 2016; 8:5941–5960. [PubMed: 26889707]
15. Tetteh G, Khan AS, Delaine-Smith RM, Reilly GC, Rehman IU. Electrospun polyurethane/hydroxyapatite bioactive scaffolds for bone tissue engineering: the role of solvent and hydroxyapatite particles. *Journal of the mechanical behavior of biomedical materials*. 2014; 39:95–110. [PubMed: 25117379]

16. Yu J, Xia H, Teramoto A, Ni QQ. Fabrication and characterization of shape memory polyurethane porous scaffold for bone tissue engineering. *Journal of biomedical materials research Part A*. 2017; 105:1132–1137. [PubMed: 28120551]
17. Zhu C, Li J, Liu C, Zhou P, Yang H, Li B. Modulation of the gene expression of annulus fibrosus-derived stem cells using poly(ether carbonate urethane)urea scaffolds of tunable elasticity. *Acta biomaterialia*. 2016; 29:228–238. [PubMed: 26432437]
18. Gomez-Lizarraga KK, Flores-Morales C, Del Prado-Audelo ML, Alvarez-Perez MA, Pina-Barba MC, Escobedo C. Polycaprolactone- and polycaprolactone/ceramic-based 3D-bioplotted porous scaffolds for bone regeneration: A comparative study. *Materials science & engineering C, Materials for biological applications*. 2017; 79:326–335. [PubMed: 28629025]
19. Kim JH, Kang MS, Eltohamy M, Kim TH, Kim HW. Dynamic Mechanical and Nanofibrous Topological Combinatory Cues Designed for Periodontal Ligament Engineering. *PloS one*. 2016; 11:e0149967. [PubMed: 26989897]
20. Kim M, Yun HS, Kim GH. Electric-field assisted 3D-fibrous bioceramic-based scaffolds for bone tissue regeneration: Fabrication, characterization, and in vitro cellular activities. *Scientific reports*. 2017; 7:3166. [PubMed: 28600540]
21. Kim W, Jang CH, Kim G. Optimally designed collagen/polycaprolactone biocomposites supplemented with controlled release of HA/TCP/rhBMP-2 and HA/TCP/PRP for hard tissue regeneration. *Materials science & engineering C, Materials for biological applications*. 2017; 78:763–772. [PubMed: 28576047]
22. Omidvar N, Ganji F, Eslaminejad MB. In vitro osteogenic induction of human marrow-derived mesenchymal stem cells by PCL fibrous scaffolds containing dexamethazone-loaded chitosan microspheres. *Journal of biomedical materials research Part A*. 2016; 104:1657–1667. [PubMed: 26916786]
23. Pobloth AM, Schell H, Petersen A, Beierlein K, Kleber C, Schmidt-Bleek K, Duda GN. Tubular open-porous beta-TCP-PLCL scaffolds as guiding structure for segmental bone defect regeneration in a novel sheep model. *Journal of tissue engineering and regenerative medicine*.
24. Thi Hiep N, Chan Khon H, Dai Hai N, Byong-Taek L, Van Toi V, Hung L Thanh. Biocompatibility of PCL/PLGA-BCP porous scaffold for bone tissue engineering applications. *Journal of biomaterials science*. 2017; 28:864–878. Polymer edition.
25. Adolph EJ, Guo R, Pollins AC, Zienkiewicz K, Cardwell N, Davidson JM, Guelcher SA, Nanney LB. Injected biodegradable polyurethane scaffolds support tissue infiltration and delay wound contraction in a porcine excisional model. *Journal of biomedical materials research*. 2016; 104:1679–1690. Part B, Applied biomaterials. [PubMed: 26343927]
26. Guo R, Ward CL, Davidson JM, Duvall CL, Wenke JC, Guelcher SA. A transient cell-shielding method for viable MSC delivery within hydrophobic scaffolds polymerized in situ. *Biomaterials*. 2015; 54:21–33. [PubMed: 25907036]
27. Hafeman AE, Zienkiewicz KJ, Carney E, Litzner B, Stratton C, Wenke JC, Guelcher SA. Local delivery of tobramycin from injectable biodegradable polyurethane scaffolds. *Journal of biomaterials science*. 2010; 21:95–112. Polymer edition.
28. Yoshii T, Hafeman AE, Esparza JM, Okawa A, Gutierrez G, Guelcher SA. Local injection of lovastatin in biodegradable polyurethane scaffolds enhances bone regeneration in a critical-sized segmental defect in rat femora. *Journal of tissue engineering and regenerative medicine*. 2014; 8:589–595. [PubMed: 22718577]
29. Yoshii T, Hafeman AE, Nyman JS, Esparza JM, Shinomiya K, Spengler DM, Mundy GR, Gutierrez GE, Guelcher SA. A sustained release of lovastatin from biodegradable, elastomeric polyurethane scaffolds for enhanced bone regeneration. *Tissue Eng Part A*. 2010; 16:2369–2379. [PubMed: 20205517]
30. Guo HC, Ye E, Li Z, Han MY, Loh XJ. Recent progress of atomic layer deposition on polymeric materials. *Materials science & engineering. C. Materials for biological applications*. 2017; 70:1182–1191. [PubMed: 27772720]
31. Li Z, Ye E, David, Lakshminarayanan R, Loh XJ. Recent Advances of Using Hybrid Nanocarriers in Remotely Controlled Therapeutic Delivery. *Small (Weinheim an der Bergstrasse, Germany)*. 2016; 12:4782–4806.

32. Loh XJ, Lee TC, Dou Q, Deen GR. Utilising inorganic nanocarriers for gene delivery. *Biomaterials science*. 2016; 4:70–86. [PubMed: 26484365]
33. Teng CP, Zhou T, Ye E, Liu S, Koh LD, Low M, Loh XJ, Win KY, Zhang L, Han MY. Effective Targeted Photothermal Ablation of Multidrug Resistant Bacteria and Their Biofilms with NIR-Absorbing Gold Nanocrosses. *Advanced healthcare materials*. 2016; 5:2122–2130. [PubMed: 27336752]
34. Ye E, Regulacio MD, Bharathi MS, Pan H, Lin M, Bosman M, Win KY, Ramanarayan H, Zhang SY, Loh XJ, Zhang YW, Han MY. An experimental and theoretical investigation of the anisotropic branching in gold nanocrosses. *Nanoscale*. 2016; 8:543–552. [PubMed: 26645742]
35. Ye E, Regulacio MD, Zhang SY, Loh XJ, Han MY. Anisotropically branched metal nanostructures. *Chemical Society reviews*. 2015; 44:6001–6017. [PubMed: 26065370]
36. Ye EY, Loh XJ. Polymeric Hydrogels and Nanoparticles: A Merging and Emerging Field. *Aust J Chem*. 2013; 66:997–1007.
37. Dou QQ, Teng CP, Ye EY, Loh XJ. Effective near-infrared photodynamic therapy assisted by upconversion nanoparticles conjugated with photosensitizers. *Int J Nanomed*. 2015; 10:419–432.
38. Ellis E, Zhang KY, Lin QY, Ye EY, Poma A, Battaglia G, Loh XJ, Lee TC. Biocompatible pH-responsive nanoparticles with a core-anchored multilayer shell of triblock copolymers for enhanced cancer therapy. *J Mat Chem B*. 2017; 5:4421–4425.
39. Teo BM, Young DJ, Loh XJ. Magnetic Anisotropic Particles: Toward Remotely Actuated Applications. *Part Part Syst Charact*. 2016; 33:709–728.
40. Dhand C, Dwivedi N, Loh XJ, Ying ANJ, Verma NK, Beuerman RW, Lakshminarayanan R, Ramakrishna S. Methods and strategies for the synthesis of diverse nanoparticles and their applications: a comprehensive overview. *RSC Adv*. 2015; 5:105003–105037.
41. Dou QQ, Fang XT, Jiang S, Chee PL, Lee TC, Loh XJ. Multi-functional fluorescent carbon dots with antibacterial and gene delivery properties. *RSC Adv*. 2015; 5:46817–46822.
42. Huang K, Dou QQ, Loh XJ. Nanomaterial mediated optogenetics: opportunities and challenges. *RSC Adv*. 2016; 6:60896–60906.
43. Lakshminarayanan R, Chi-Jin EO, Loh XJ, Kini RM, Valiyaveetil S. Purification and characterization of a vaterite-inducing peptide, pelovaterin, from the eggshells of *Pelodiscus sinensis* (Chinese soft-shelled turtle). *Biomacromolecules*. 2005; 6:1429–1437. [PubMed: 15877362]
44. Lakshminarayanan R, Loh XJ, Gayathri S, Sindhu S, Banerjee Y, Kini RM, Valiyaveetil S. Formation of transient amorphous calcium carbonate precursor in quail eggshell mineralization: an in vitro study. *Biomacromolecules*. 2006; 7:3202–3209. [PubMed: 17096552]
45. Neumann AJ, Alini M, Archer CW, Stoddart MJ. Chondrogenesis of human bone marrow-derived mesenchymal stem cells is modulated by complex mechanical stimulation and adenoviral-mediated overexpression of bone morphogenetic protein 2. *Tissue Eng Part A*. 2013; 19:1285–1294. [PubMed: 23289669]
46. Neumann AJ, Gardner OF, Williams R, Alini M, Archer CW, Stoddart MJ. Human Articular Cartilage Progenitor Cells Are Responsive to Mechanical Stimulation and Adenoviral-Mediated Overexpression of Bone-Morphogenetic Protein 2. *PLoS one*. 2015; 10:e0136229. [PubMed: 26292283]
47. Hafeman AE, Li B, Yoshii T, Zienkiewicz K, Davidson JM, Guelcher SA. Injectable biodegradable polyurethane scaffolds with release of platelet-derived growth factor for tissue repair and regeneration. *Pharmaceutical research*. 2008; 25:2387–2399. [PubMed: 18516665]
48. Chen Z, Cheng S, Li Z, Xu K, Chen GQ. Synthesis, characterization and cell compatibility of novel poly(ester urethane)s based on poly(3-hydroxybutyrate-co-4-hydroxybutyrate) and poly(3-hydroxybutyrate-co-3-hydroxyhexanoate) prepared by melting polymerization. *Journal of biomaterials science*. 2009; 20:1451–1471. Polymer edition.
49. Guan J, Fujimoto KL, Sacks MS, Wagner WR. Preparation and characterization of highly porous, biodegradable polyurethane scaffolds for soft tissue applications. *Biomaterials*. 2005; 26:3961–3971. [PubMed: 15626443]

50. Guan J, Wagner WR. Synthesis, characterization and cytocompatibility of polyurethaneurea elastomers with designed elastase sensitivity. *Biomacromolecules*. 2005; 6:2833–2842. [PubMed: 16153125]
51. Hong Y, Guan J, Fujimoto KL, Hashizume R, Pelinescu AL, Wagner WR. Tailoring the degradation kinetics of poly(ester carbonate urethane)urea thermoplastic elastomers for tissue engineering scaffolds. *Biomaterials*. 2010; 31:4249–4258. [PubMed: 20188411]
52. Wang F, Li Z, Lannutti JL, Wagner WR, Guan J. Synthesis, characterization and surface modification of low moduli poly(ether carbonate urethane)ureas for soft tissue engineering. *Acta biomaterialia*. 2009; 5:2901–2912. [PubMed: 19433136]
53. Wang Q, Chen C, Liu W, He X, Zhou N, Zhang D, Gu H, Li J, Jiang J, Huang W. Levofloxacin loaded mesoporous silica microspheres/nano-hydroxyapatite/polyurethane composite scaffold for the treatment of chronic osteomyelitis with bone defects. *Scientific reports*. 2017; 7:41808. [PubMed: 28150731]
54. Yang W, Both SK, van Osch GJ, Wang Y, Jansen JA, Yang F. Performance of different three-dimensional scaffolds for in vivo endochondral bone generation. *European cells & materials*. 2014; 27:350–364. [PubMed: 24913441]
55. Das B, Chattopadhyay P, Maji S, Upadhyay A, Purkayastha M Das, Mohanta CL, Maity TK, Karak N. Bio-functionalized MWCNT/hyperbranched polyurethane bionanocomposite for bone regeneration. *Biomedical materials (Bristol, England)*. 2015; 10:025011.
56. Han Z, Kong H, Meng J, Wang C, Xie S, Xu H. Electrospun aligned nanofibrous scaffold of carbon nanotubes-polyurethane composite for endothelial cells. *Journal of nanoscience and nanotechnology*. 2009; 9:1400–1402. [PubMed: 19441533]
57. Mi HY, Jing X, Salick MR, Cordie TM, Turng LS. Carbon nanotube (CNT) and nanofibrillated cellulose (NFC) reinforcement effect on thermoplastic polyurethane (TPU) scaffolds fabricated via phase separation using dimethyl sulfoxide (DMSO) as solvent. *Journal of the mechanical behavior of biomedical materials*. 2016; 62:417–427. [PubMed: 27266475]
58. Bakhtiyari SS, Karbasi S, Monshi A, Montazeri M. Evaluation of the effects of nano-TiO₂ on bioactivity and mechanical properties of nano bioglass-P3HB composite scaffold for bone tissue engineering. *Journal of materials science. Materials in medicine*. 2016; 27:2. [PubMed: 26610925]
59. Pourmollaabbassi B, Karbasi S, Hashemibeni B. Evaluate the growth and adhesion of osteoblast cells on nanocomposite scaffold of hydroxyapatite/titania coated with poly hydroxybutyrate. *Advanced biomedical research*. 2016; 5:156. [PubMed: 27761431]
60. Paul DR, Robeson LM. Polymer nanotechnology: Nanocomposites. *Polymer*. 2008; 49:3187–3204.
61. Borzabadi-Farahani A, Borzabadi E, Lynch E. Nanoparticles in orthodontics, a review of antimicrobial and anti-caries applications. *Acta odontologica Scandinavica*. 2014; 72:413–417. [PubMed: 24325608]
62. Cheng L, Zhang K, Weir MD, Melo MA, Zhou X, Xu HH. Nanotechnology strategies for antibacterial and remineralizing composites and adhesives to tackle dental caries. *Nanomedicine (London, England)*. 2015; 10:627–641.
63. Gulati K, Ivanovski S. Dental implants modified with drug releasing titania nanotubes: therapeutic potential and developmental challenges. *Expert opinion on drug delivery*.
64. Rehman FU, Zhao C, Jiang H, Wang X. Biomedical applications of nano-titania in theranostics and photodynamic therapy. *Biomaterials science*. 2016; 4:40–54. [PubMed: 26442645]
65. Charpentier PA, Burgess K, Wang L, Chowdhury RR, Lotus AF, Moula G. Nano-TiO₂/polyurethane composites for antibacterial and self-cleaning coatings. *Nanotechnology*. 2012; 23:425606. [PubMed: 23037881]
66. Chen Z, Wang Y, Ba T, Li Y, Pu J, Chen T, Song Y, Gu Y, Qian Q, Yang J, Jia G. Genotoxic evaluation of titanium dioxide nanoparticles in vivo and in vitro. *Toxicology letters*. 2014; 226:314–319. [PubMed: 24594277]
67. Diez-Pascual AM, Diez-Vicente AL. Nano-TiO₂ reinforced PEEK/PEI blends as biomaterials for load-bearing implant applications. *ACS applied materials & interfaces*. 2015; 7:5561–5573. [PubMed: 25706225]

68. Smith IO, Liu XH, Smith LA, Ma PX. Nanostructured polymer scaffolds for tissue engineering and regenerative medicine, Wiley interdisciplinary reviews. Nanomedicine and nanobiotechnology. 2009; 1:226–236. [PubMed: 20049793]
69. Sun H, Feng K, Hu J, Soker S, Atala A, Ma PX. Osteogenic differentiation of human amniotic fluid-derived stem cells induced by bone morphogenetic protein-7 and enhanced by nanofibrous scaffolds. Biomaterials. 2010; 31:1133–1139. [PubMed: 19857889]
70. Wang J, Liu X, Jin X, Ma H, Hu J, Ni L, Ma PX. The odontogenic differentiation of human dental pulp stem cells on nanofibrous poly(L-lactic acid) scaffolds in vitro and in vivo. Acta biomaterialia. 2010; 6:3856–3863. [PubMed: 20406702]
71. Wang W, Dang M, Zhang Z, Hu J, Eyster TW, Ni L, Ma PX. Dentin regeneration by stem cells of apical papilla on injectable nanofibrous microspheres and stimulated by controlled BMP-2 release. Acta biomaterialia. 2016; 36:63–72. [PubMed: 26971664]
72. Borteh HM, Gallovic MD, Sharma S, Peine KJ, Miao S, Brackman DJ, Gregg K, Xu Y, Guo X, Guan J, Bachelder EM, Ainslie KM. Electrospun acetalated dextran scaffolds for temporal release of therapeutics. Langmuir : the ACS journal of surfaces and colloids. 2013; 29:7957–7965. [PubMed: 23725054]
73. Guo X, Elliott CG, Li Z, Xu Y, Hamilton DW, Guan J. Creating 3D angiogenic growth factor gradients in fibrous constructs to guide fast angiogenesis. Biomacromolecules. 2012; 13:3262–3271. [PubMed: 22924876]
74. Wang F, Li Z, Tamama K, Sen CK, Guan J. Fabrication and characterization of pro-survival growth factor releasing, anisotropic scaffolds for enhanced mesenchymal stem cell survival/growth and orientation. Biomacromolecules. 2009; 10:2609–2618. [PubMed: 19689108]
75. Xu Y, Patnaik S, Guo X, Li Z, Lo W, Butler R, Claude A, Liu Z, Zhang G, Liao J, Anderson PM, Guan J. Cardiac differentiation of cardiosphere-derived cells in scaffolds mimicking morphology of the cardiac extracellular matrix. Acta biomaterialia. 2014; 10:3449–3462. [PubMed: 24769114]
76. Zhang CL, Yu SH. Nanoparticles meet electrospinning: recent advances and future prospects. Chemical Society reviews. 2014; 43:4423–4448. [PubMed: 24695773]
77. Wang F, Li Z, Guan J. Fabrication of mesenchymal stem cells-integrated vascular constructs mimicking multiple properties of the native blood vessels. Journal of biomaterials science. 2013; 24:769–783. Polymer edition.
78. Nune KC, Misra RD, Li SJ, Hao YL, Yang R. Cellular response of osteoblasts to low modulus Ti-24Nb-4Zr-8Sn alloy mesh structure. Journal of biomedical materials research. 2017; 105:859–870. Part A. [PubMed: 27885781]
79. Xu Y, Fu M, Li Z, Fan Z, Li X, Liu Y, Anderson PM, Xie X, Liu Z, Guan J. A pro-survival and pro-angiogenic stem cell delivery system to promote ischemic limb regeneration. Acta biomaterialia. 2016; 31:99–113. [PubMed: 26689466]
80. Xu Y, Li Z, Li X, Fan Z, Liu Z, Xie X, Guan J. Regulating myogenic differentiation of mesenchymal stem cells using thermosensitive hydrogels. Acta biomaterialia. 2015; 26:23–33. [PubMed: 26277379]
81. Gratzel M. Solar energy conversion by dye-sensitized photovoltaic cells. Inorg Chem. 2005; 44:6841–6851. [PubMed: 16180840]
82. Jing Z, Wu Y, Su W, Tian M, Jiang W, Cao L, Zhao L, Zhao Z. Carbon Nanotube Reinforced Collagen/Hydroxyapatite Scaffolds Improve Bone Tissue Formation In Vitro and In Vivo. Annals of biomedical engineering.
83. Loberg J, Holmberg J, Perez, Mattisson I, Arvidsson A, Ahlberg E. Electronic Properties of TiO₂ Nanoparticles Films and the Effect on Apatite-Forming Ability. International journal of dentistry. 2013; 2013:139615. [PubMed: 23737786]
84. Nogueiras R, Habegger KM, Chaudhary N, Finan B, Banks AS, Dietrich MO, Horvath TL, Sinclair DA, Pfluger PT, Tschöp MH. Sirtuin 1 and sirtuin 3: physiological modulators of metabolism. Physiological reviews. 2012; 92:1479–1514. [PubMed: 22811431]

Highlights

- Grafted degradable polyurethane into TiO₂ nanoparticles;
- Modified TiO₂ nanoparticles reinforced fibrous polyurethane scaffolds;
- Reinforced scaffolds promoted biomineralization and stem cell proliferation.

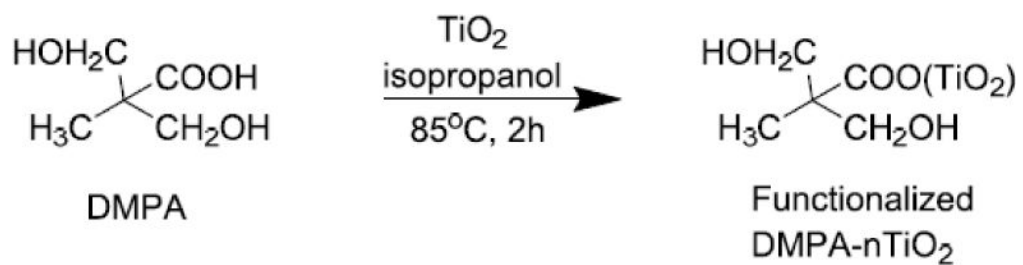


Figure 1.
Synthesis of DMPA functionalized TiO₂ nanoparticles (DMPA-nTiO₂).

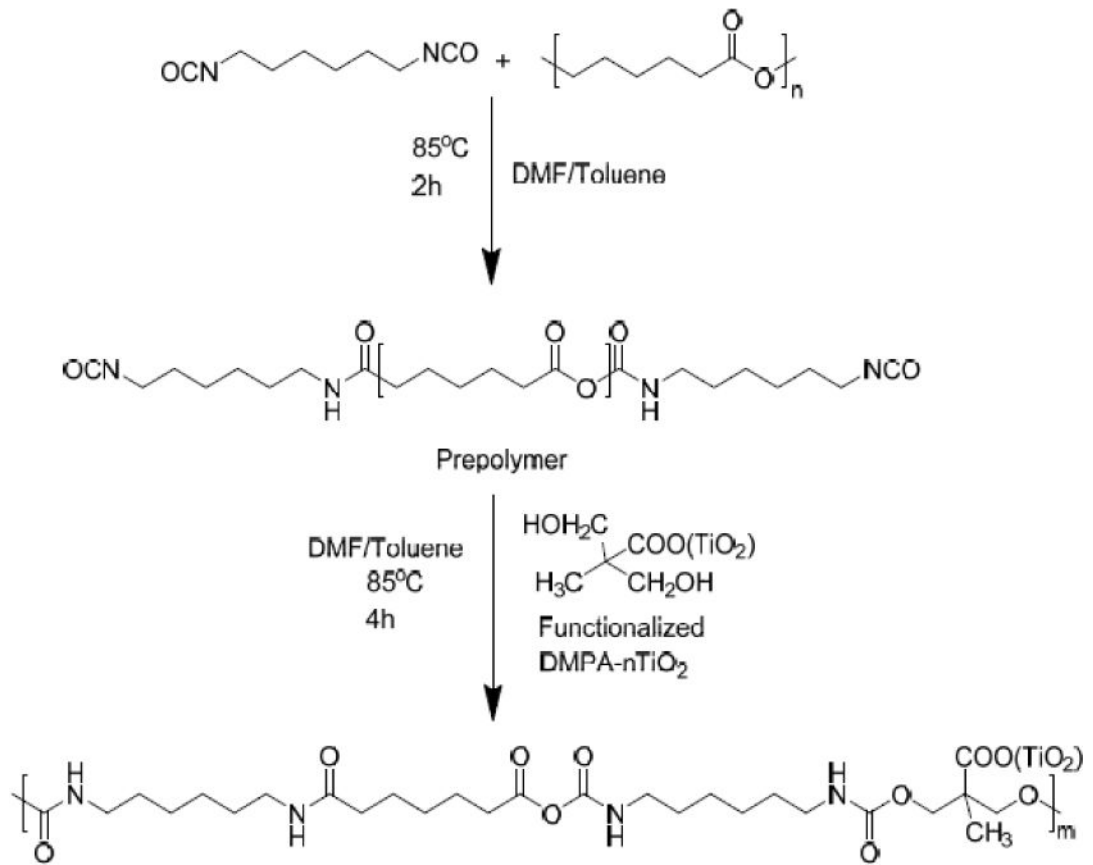


Figure 2. Synthesis of degradable polyurethane conjugated with TiO_2 nanoparticles (PEU-g- $n\text{TiO}_2$).

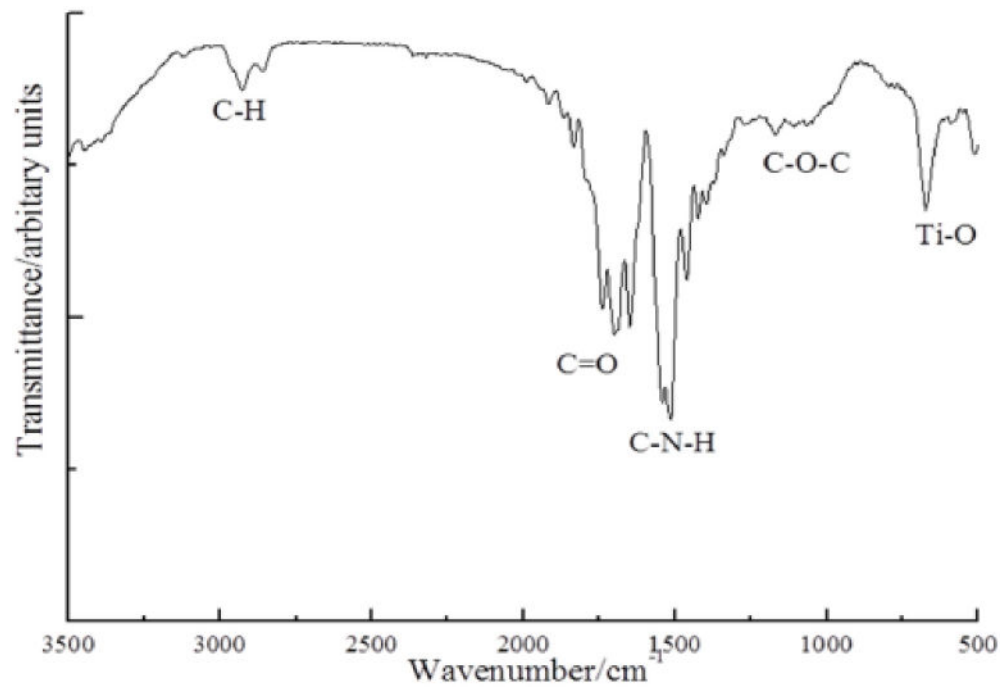


Figure 3.
FTIR spectrum of synthesized PEU-g-nTiO₂.

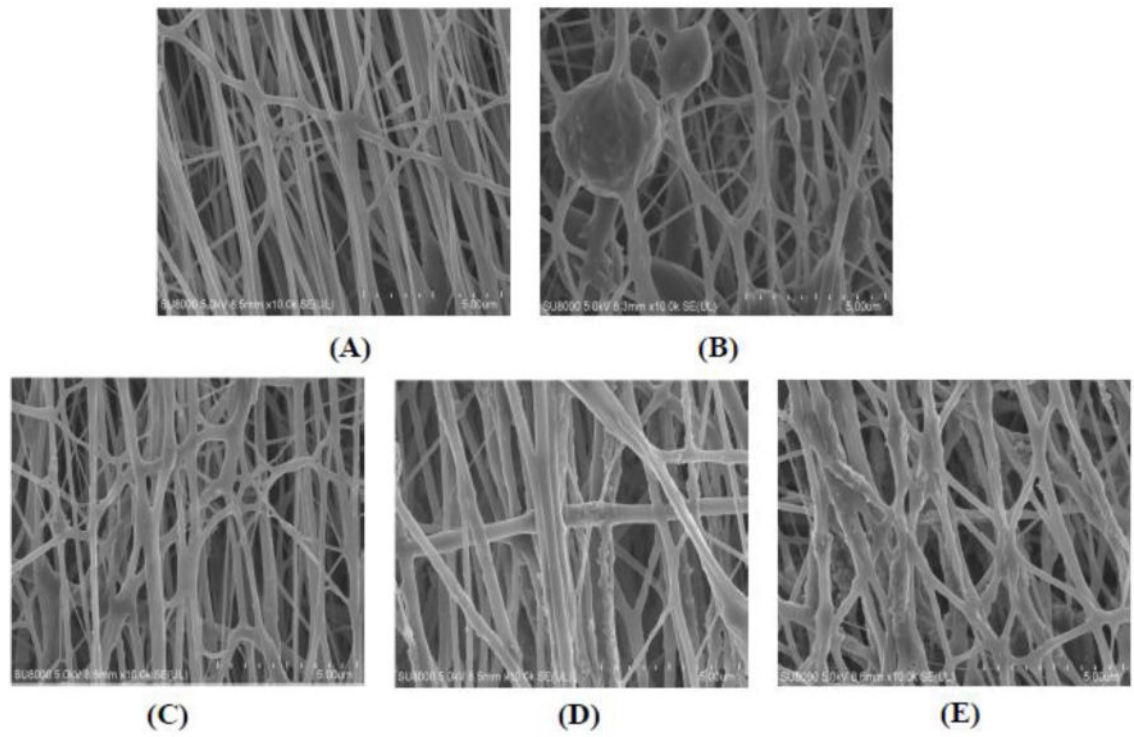


Figure 4. Morphology of the electrospun scaffolds. (A) PEUU; (B) nTiO₂/PEUU; (C) PEU-g-nTiO₂/PEUU=1:2; (D) PEU-g-nTiO₂/PEUU=1:1; and (E) PEU-g-nTiO₂/PEUU=2:1.

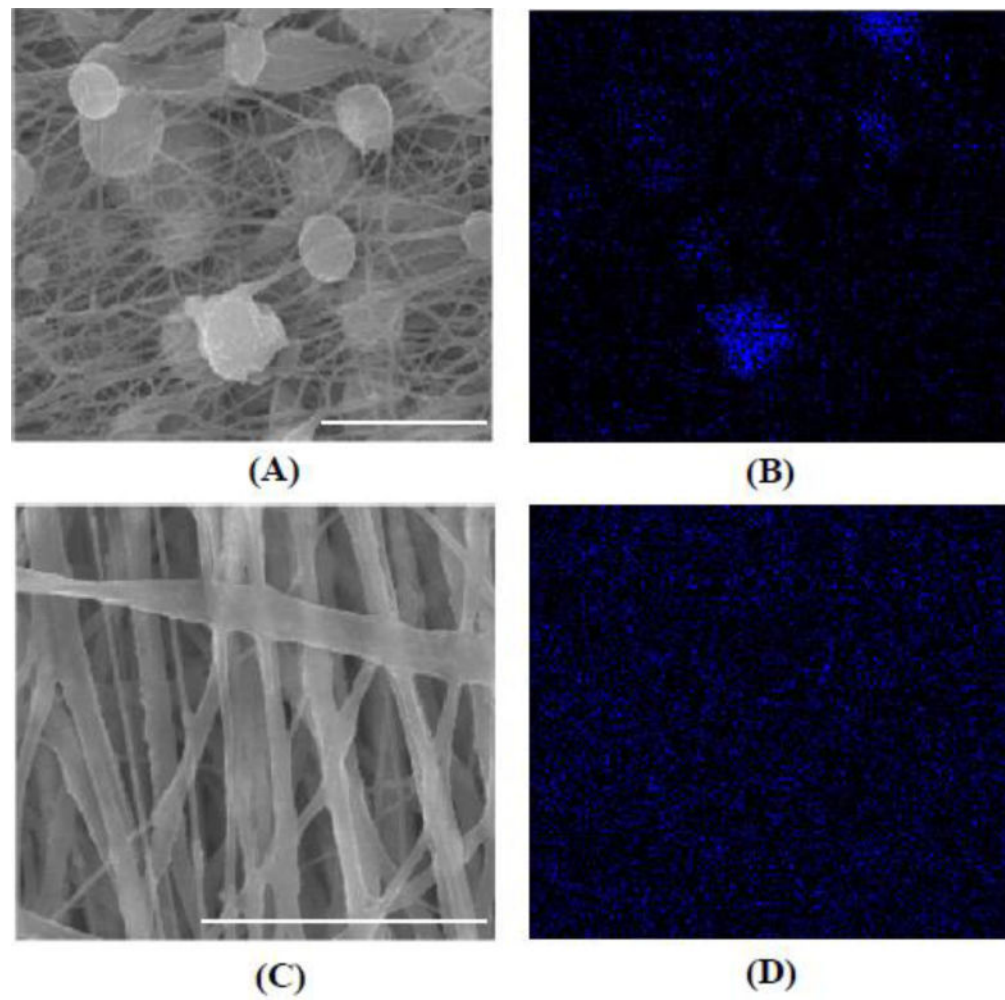


Figure 5. SEM images (A, C) and corresponding EDX analysis of Ti distribution in the scaffolds (B, D). (A, B) nTiO₂/PEUU; (C, D) PEU-g-nTiO₂/PEUU=2/1. Scale bar = 5 μ m.

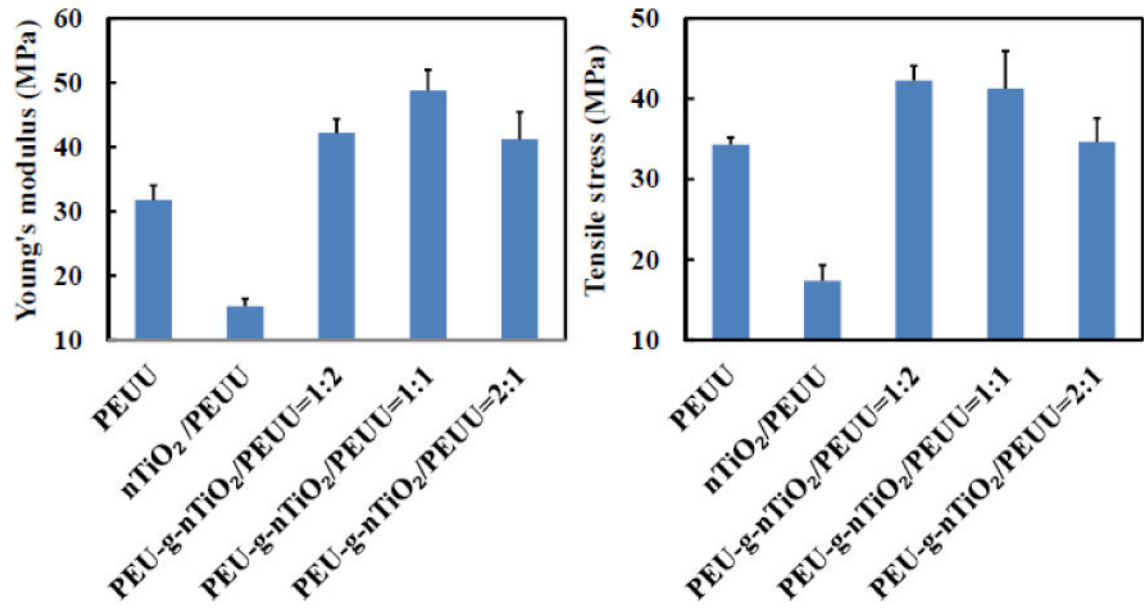


Figure 6. Mechanical properties of electrospun scaffolds with and without reinforcement with PEU-gnTiO₂.

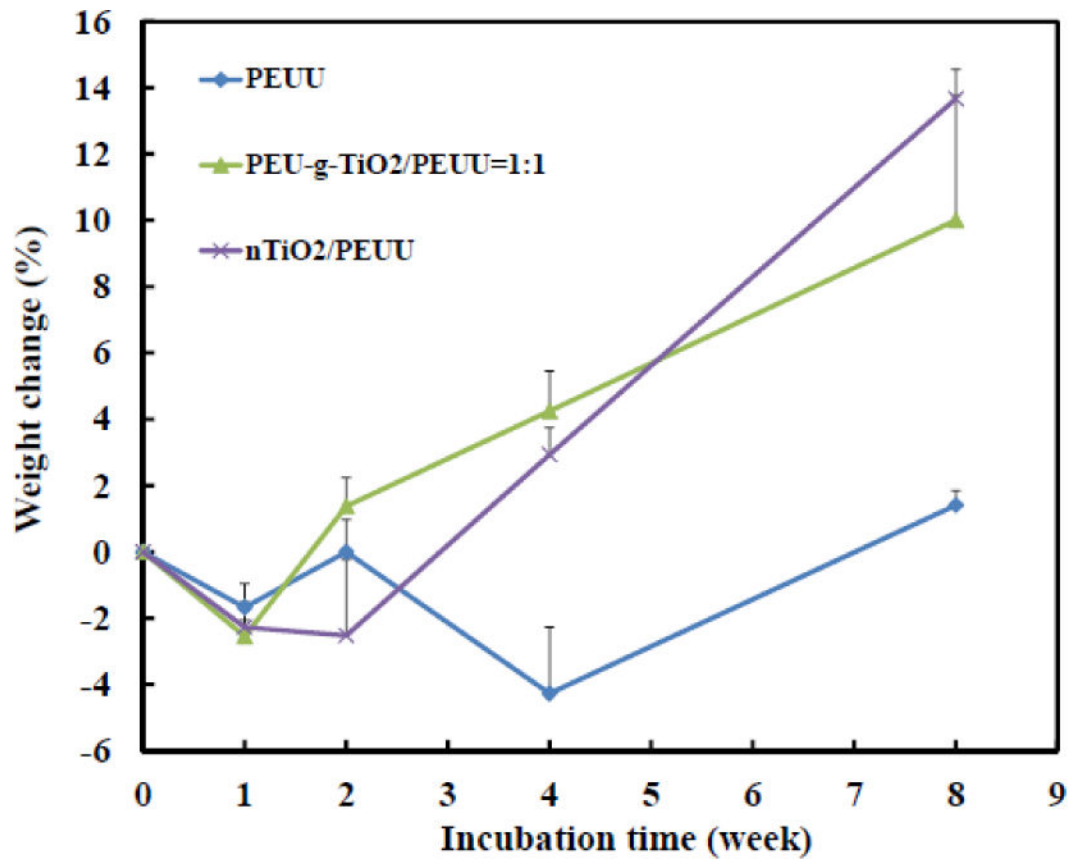


Figure 7. Weight change of scaffolds incubated in the 37°C simulated body fluid for 8 weeks.

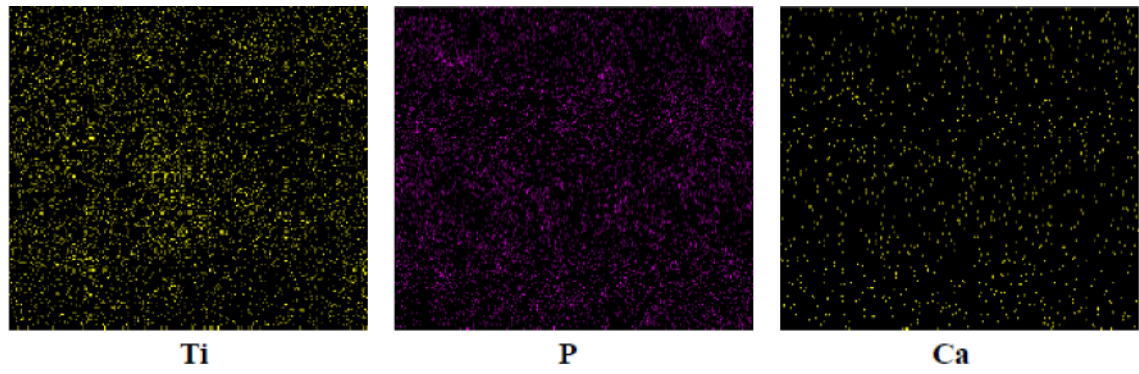


Figure 8.
EDX characterization of Ca and P deposition in the scaffold PEU-g-nTiO₂/PEUU = 1:1.

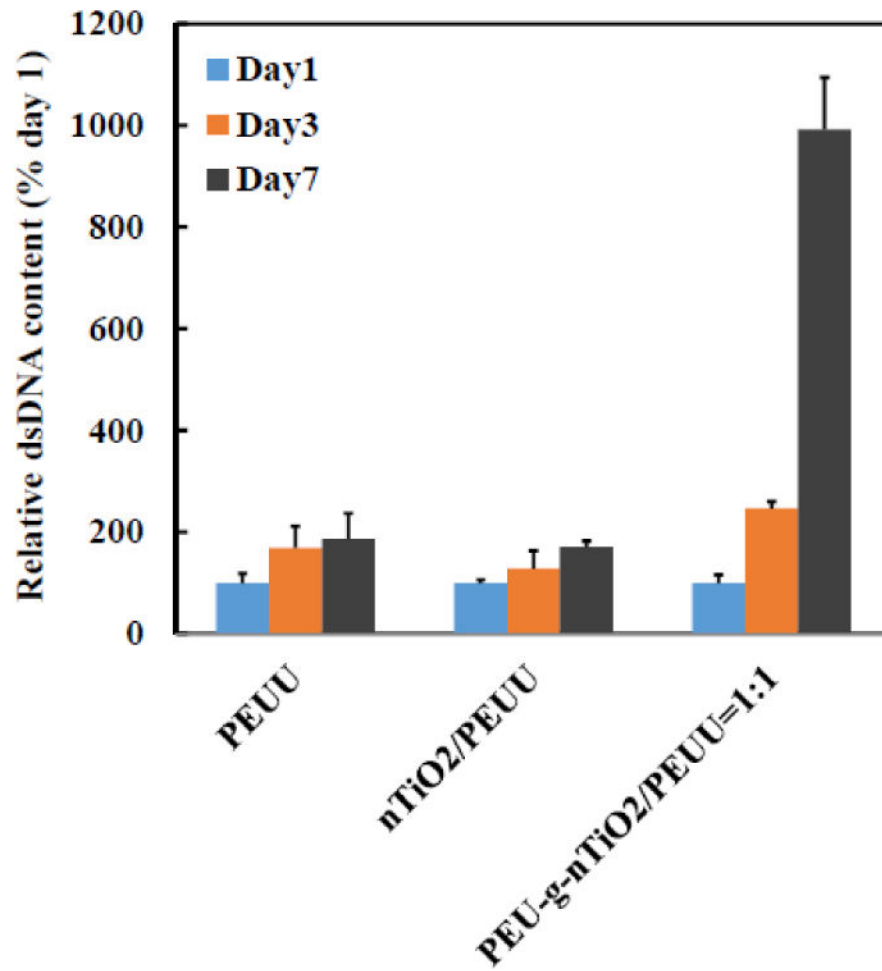


Figure 9. Mesenchymal stem cell growth on the scaffolds with and without reinforcement with PEU-gnTiO₂.

Table 1

EDX analysis of Ca and P content in the scaffolds after 8 weeks of incubation in SBF.

Element (%)	PEUU	nTiO ₂ /PEUU	PEU-g-TiO ₂ /PEUU
Ca	0.039	0.103	0.203
P	0.143	0.327	1.270

Author Manuscript

Author Manuscript

Author Manuscript

Author Manuscript